Remote Sensing of Environment 194 (2017) 401–411

Contents lists available at ScienceDirect

Remote Sensing of Environment

journal homepage: www.elsevier.com/locate/rse

Seasonal and interannual variability of the Douro turbid river plume, northwestern Iberian Peninsula

Renato Mendes [a,*], Gonzalo S. Saldías [b,c], Maite deCastro [d], Moncho Gómez-Gesteira [d], Nuno Vaz [a], João Miguel Dias [a]

[a] CESAM, Departamento de Física, Universidade de Aveiro, 3810-193 Aveiro, Portugal
[b] College of Earth, Ocean, and Atmospheric Sciences, Oregon State University, Corvallis, OR, USA
[c] Centro FONDAP de Investigación en Dinámica de Ecosistemas Marinos de Altas Latitudes (IDEAL), Valdivia, Chile
[d] EPhysLab (Environmental Physics Laboratory), Universidade de Vigo, Facultade de Ciencias, Ourense, Spain

ARTICLE INFO

Article history:
Received 17 February 2016
Received in revised form 10 March 2017
Accepted 5 April 2017
Available online xxxx

Keywords:
River plumes
MODIS imagery
Teleconnection indices
NW Iberian Peninsula

ABSTRACT

The Douro River represents the major freshwater input into the coastal ocean of the northwestern Iberian Peninsula. The seasonal and interannual variability of its turbid plume is investigated using ocean color composites from MODIS (Moderate Resolution Imaging Spectroradiometer) sensor aboard the Aqua and Terra satellites (2000–2014) and long-term records of river discharge, wind and precipitation rate. Regional climate indices, namely the Eastern Atlantic (EA) and North Atlantic Oscillation (NAO), were analyzed to identify the influence of atmospheric variability on the generation of anomalous turbid river plume patterns. The connection between the monthly time series of normalized water leaving radiance at 555 nm (*nLw(555)*) and river discharge is high ($r = 0.81$), which indicates a strong link between river outflow and turbidity levels in the river plume. The equivalent result is found between precipitation and *nLw(555)* time series, but the peak correlation was found with a 1-month lag, revealing the importance of the river dams on the outflow regulation ($r = 0.65$). Lag correlations between *nLw(555)* and EA index show a peak at 1-month lag ($r = 0.51$). The relation between NAO index and Douro river discharge is considerable (-0.50), for a time lag of 1-month as well. However, the correlation coefficient between *nLw(555)* and NAO index presents a maximum peak for a longer period ($r = -0.42$ at 3-month). Anomalous turbid plume patterns, not related with estuarine outflow, are found during autumn 2004. A coccolithophore bloom is proposed as a plausible explanation for these unexpected turbid patches.

1. Introduction

River plumes are closely associated with a wide range of physical and biogeochemical shelf processes near river mouths (Dyer, 1973; Dzwonkowski and Yan, 2005). The spreading and variability of buoyant plumes depend on complex interactions among topographic constraints, ambient flow and high variability of dominant forcing: river discharge, wind stress, Coriolis effect and tides (Fong and Geyer, 2001; García Berdeal et al., 2002; Garvine, 1974; Hetland, 2005; Horner-Devine et al., 2015; Yankovsky and Chapman, 1997). The high variability of the main driver, i.e. freshwater discharge, often results in significant structural and dynamical differences among river plumes (Horner-Devine et al., 2015).

Some studies along the NW Iberian Peninsula have highlighted the importance of river runoff and estuarine plumes on local coastal circulation patterns (Peliz et al., 2002; Relvas et al., 2007; Santos et al., 2004; Torres and Barton, 2007). The freshwater discharge presents a marked annual cycle, with peak values during winter and lower flow during summer (Azevedo et al., 2008; Mendes et al., 2014). These seasonal fluctuations produce a variable estuarine outflow that modulates coastal circulation and biogeochemistry in the region (Picado et al., 2014) – the river outflow is a major supplier of sediment and nutrients into the coastal ocean. Moreover, the Douro estuarine plume is the major contributor to the Western Iberian Buoyant Plume (WIBP), which is an accumulation of a less dense water mass originated from all river outflows along the northern Portuguese coast that under persistent downwelling-favorable wind conditions flows northward as a classic coastal-attached buoyant plume (Mendes et al., 2016; Otero et al., 2008, 2009; Santos et al., 2004).

The Douro River is 927 km long, drains to the NW coast of Portugal and has a catchment basin that is the largest in the Iberian Peninsula (97,682 km^2). The Douro estuary is 21.6 km long, being delimited upstream by a dam that leads to an artificial separation from the river (Fig. 1). The daily mean freshwater discharge ranges from zero to >13,000 $m^3\ s^{-1}$ (Azevedo et al., 2010), with an average of 708 $m^3\ s^{-1}$. Rainfall episodes enhance river plume outflow, with a significant supply of nutrients and suspended matter to the continental

* Corresponding author.
E-mail address: rpsm@ua.pt (R. Mendes).

http://dx.doi.org/10.1016/j.rse.2017.04.001
0034-4257/

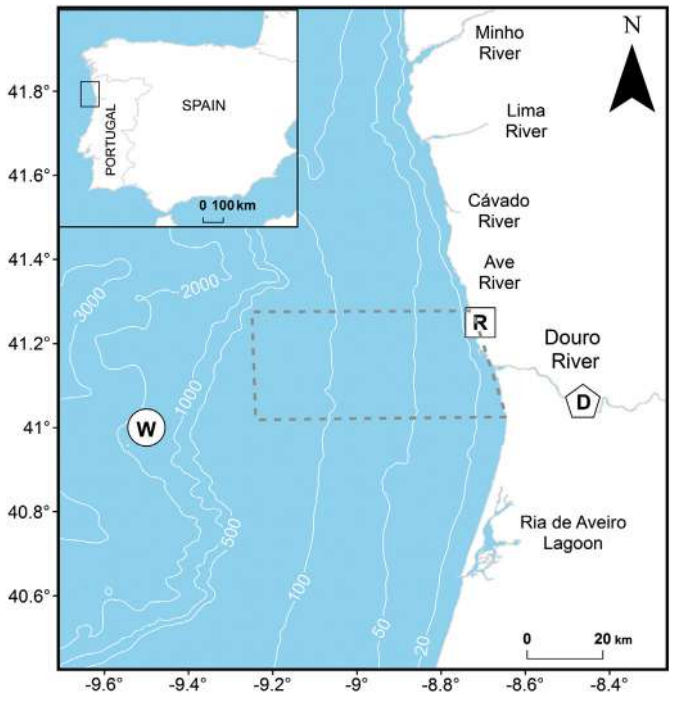

Fig. 1. Study area with location of the main rivers near the interest point (Lima, Cávado, and Ave rivers and Ria de Aveiro coastal lagoon). Wind and precipitation data stations are marked with a white circle (W) and square (R), respectively. The black pentagon (D) represents the location of the downstream Douro River dam. The dashed black box near the river mouth represents the near-field area of Douro River influence. Bathymetry, from General Bathymetric Chart of the Oceans (GEBCO), is shown with white lines (contours in meters).

shelf. The Douro River delivers about 87% of the fluvial sediments discharged into the NW Iberian coast (Dias, 1987) and the current deficit of sediments discharged by its estuary is commonly referred as a primary reason for severe erosion along southward beaches (Dias, 1990; Oliveira et al., 1982; Veloso-Gomes et al., 2004). Douro River runoff also poses a particular relevance on the coastal biogeochemistry, in particular during upwelling winter events (Picado et al., 2014; Prego et al., 2007; Ribeiro et al., 2005; Santos et al., 2004). Also, vertical stratification, enhanced by the plume, plays a key role on larvae retention (Santos et al., 2004). In these upwelling winter events, buoyant water (rich in nutrients) stimulates phytoplankton growth (Chícharo et al., 2003; Prego et al., 2007; Santos et al., 2004), contributing to an increase of primary production. Recently, Mendes et al. (2014) described the mean-state patterns of the Douro River plume through ocean color imagery, highlighting that the turbid plume is readily detected when the river flow exceeds 500 $m^3\ s^{-1}$. River discharge and wind are the main drivers of the plume, whereas tidal effect is most important near the estuary mouth. An offshore plume expansion is observed under northerly winds and high river discharges. A northward coastal-attached plume is commonly observed under downwelling-favorable winds. An offshore plume detached from the coast is observed under seaward winds, while westerly winds (onshore) tend to favor the freshwater accumulation near shore and to decrease the cross-shore advection (Mendes et al., 2014).

The Eastern Atlantic (EA) and North Atlantic Oscillation (NAO) are two of the most representative regional patterns of atmospheric variation in the Northern Hemisphere, impacting the local precipitation and river discharges, and with higher amplitude during winter (deCastro et al., 2008a, b; deCastro et al., 2006a, b; Lorenzo and Taboada, 2005; Trigo et al., 2004; Zorita et al., 1992). Several works have shown a significant correlation between NAO index and precipitation in Galicia during winter (northwest of Iberian Peninsula) (Esteban-Parra et al., 1998; Lorenzo and Taboada, 2005; Zorita et al., 1992). Trigo et al. (2004) found that river discharge is significantly correlated with the NAO index in winter (for the period 1973–1998) with a 1-month lag peak (−0.76 for Douro, −0.77 for the Tagus and −0.79 for the Guadiana river). Furthermore, deCastro et al. (2006a, b) found significant correlations between Minho river discharge and (DJF) NAO index for the period 1970–2005 with a 2-month lag peak, showing a decreased correlation in the last years, which is in agreement with the decreased trend in spatial correlation found by Trigo et al. (2004). Regarding EA variability, Rodriguez-Puebla et al. (1998) found correlation with the annual precipitation for Iberian Peninsula for April EA, while deCastro et al. (2006a, b) showed a negative correlation between Minho River discharge and (DJF) EA with a peak at 1-month lag. In addition, they are connected to different types of wind patterns, which influence the plume propagation. Upwelling along this area is a frequent phenomenon during the spring–summer months, when northerly winds prevail along the shelf. However, persistent northern and northeasterly winds are also observed during winter, inducing upwelling events (Álvarez et al., 2009; deCastro et al., 2008a, b), with similar patterns to those observed during summer, when precipitation and river discharge are minimum.

The Douro estuarine plume was studied by Mendes et al. (2014) to obtain a synoptic picture of the propagation of the plume using satellite imagery. However, no previous investigation is available on how this estuarine plume is influenced by changes in the main forcing from winter to summer conditions or even during peak freshwater discharge and wind. This study intends to be a step forward in the study of the Douro Estuarine plume at seasonal and interannual scales of variability, and their relationship with the atmospheric forcing.

Data and methods are described in Section 2. The results and discussion are presented in Section 3, highlighting the dominant spatio-temporal plume patterns along the coast and their connection with wind and climate indices at interannual scale. Finally, the principal conclusions are presented in Section 4.

2. Data and methods

2.1. Ocean color imagery

Satellite ocean color imagery provides unique information for detecting and monitoring the Douro River plume (e.g. Mendes et al., 2014). In general, ocean color images allow the resolution of submesoscale to small-scale features in river plumes (Aurin et al., 2013). The ocean color signal of river plumes, due to their high turbidity, is often well correlated with surface salinity, which is the natural tracer of freshwater buoyant plumes (e.g. Binding and Bowers, 2003; Burrage et al., 2008; Klemas, 2011; Molleri et al., 2010; Palacios et al., 2009; Piola et al., 2008; Saldías et al., 2016a). Thus, satellite-derived turbidity patterns become a direct proxy to identify river plumes on coastal areas (Fernández-Nóvoa et al., 2015; Mendes et al., 2014; Nezlin et al., 2005; Saldías et al., 2012; Saldías et al., 2016b).

All full-resolution L1A files from MODIS-Aqua and MODIS-Terra covering the Douro Estuary region (swaths inside the box 40°–43°N; 11°–7.5°W) and available from NASA (http://oceancolor.gsfc.nasa.gov) were used in this study. As MODIS imagery from Aqua is available from July 2002, previous data (Feb. 2000–Jun. 2002) correspond solely to MODIS-Terra. L1A files were processed using the SeaDAS (SeaWIFS Data Analysis System, version 6.4, Baith et al., 2001) software, following standard procedures for processing raw data files. L1B files were then converted to L2 files by applying a methodology similar to that provided by Mendes et al. (2014). The processing generates high-resolution (~500 m) daily *nLw(555)* (normalized water-leaving radiance at 555 nm; mW $cm^{-2}\ m^{-1}\ sr^{-1}$) images from February 2000 to December 2014. Swaths were mapped into a regular lat-lon grid (0.005° × 0.005°) and daily averaged images were generated when more than one existed for the same day. From all visible spectrum bands available in MODIS, the *nLw(555)* is the best proxy for mapping the Douro river plume – it

presents high correlation with the river discharge and, in addition, there is increased percentage of valid daily images to study the turbid river plume (Mendes et al., 2014). Moreover, small differences between Aqua and Terra data for green channels (Franz et al., 2006) allow merging the *nLw(555)* images from both platforms in this region (Mendes et al., 2014). The average and standard deviation of *nLw(555)* in the Douro region from Aqua, Terra, and merged data from both satellites are depicted in Fig. 2. Differences in long-term averages and standard deviation are minor between platforms and the merged product - high standard deviation values are restricted to the pixels near the Douro River mouth where the turbid plume has a major impact (Fig. 2d, e, f). Merged data, however, presents a considerable increase of daily available pixels (Fig. 2i). Using *nLw(555)* merged data results in a maximum of 40–45% of cloud-free data along the coast, whereas the available data is greatly reduced to 25–35% in single cases from Aqua or Terra (Fig. 2g–h). Then, *nLw(555)* merged composites were monthly averaged to guarantee >99% of good data in the entire study area and, at the same time, to study the interannual variability of the Douro turbid river plume.

Different methods could be used, as the criterion of plume intensity, to compare the temporal variation of the Douro turbid river plume obtained from satellite-derived turbidity with environmental information from other datasets. The monthly average of *nLw(555)*, the number of turbid pixels NTP (>1.1 mW cm^{-2} μm^{-1} sr^{-1}, Mendes et al., 2014), and the product between the NTP and the averaged *nLw(555)* are presented in Fig. 3 within a box close to river mouth (dashed line in Fig. 1 – 41.02°–41.25°N; 9.25°–8.69°W). The *nLw(555)* criterion to define plume regions can be considered subjective, as pointed out by Mendes et al. (2014) in their work about Douro plume as well as by additional authors (i.e. Nezlin et al., 2005; Saldías et al., 2012) for other river plume studies. However, the application of these methods is adequate to quantify the area of a plume and to define its spatial limits at daily scales, having the potential to mask occasional plume events during

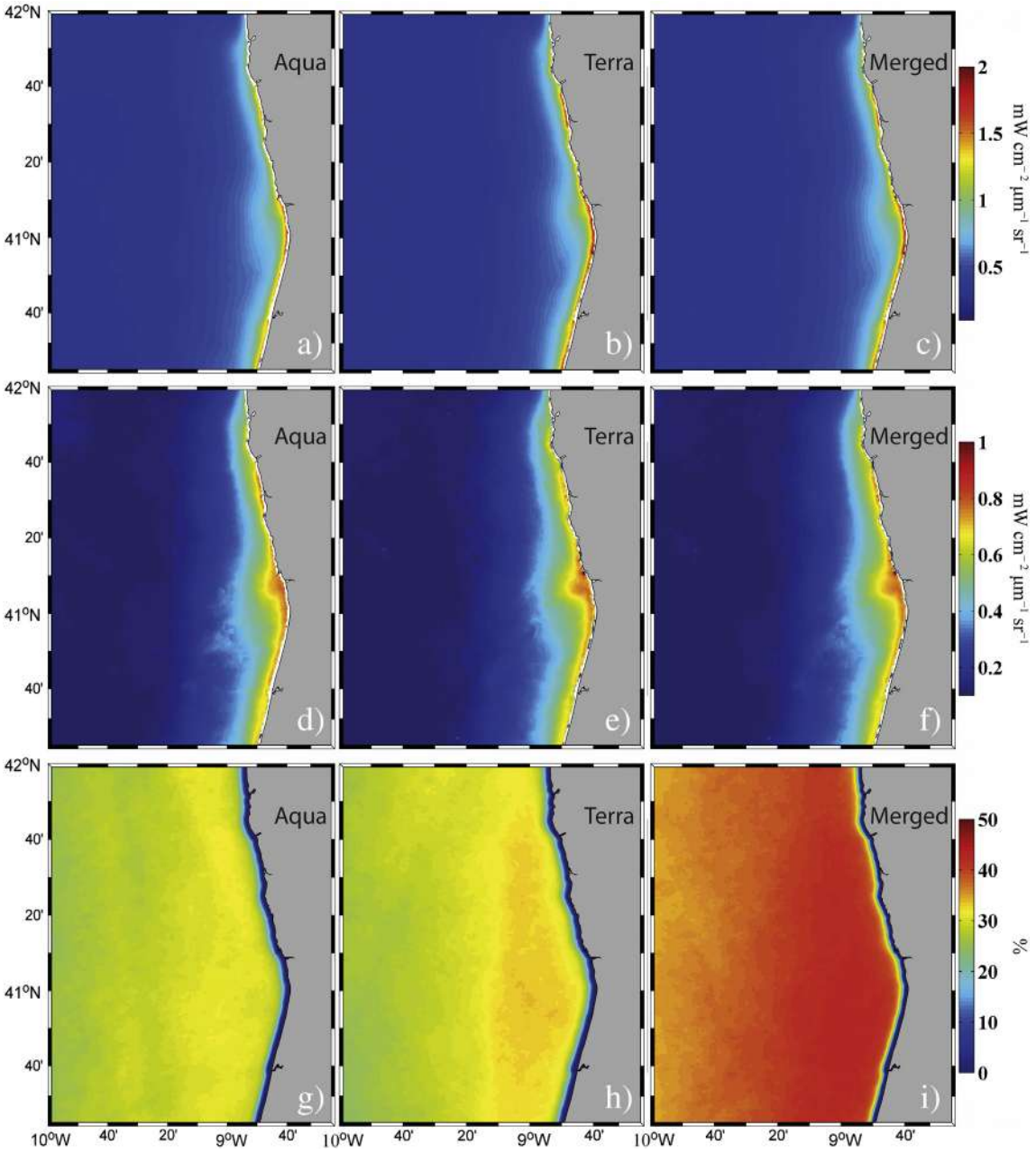

Fig. 2. (upper panels) Averages, (middle panels in the vertical direction) standard deviations, and (lower panels) percentage of daily cloud-free data of *nLw(555)* from (left panels) MODIS-Aqua, (middle panels in the horizontal direction) MODIS-Terra, and (right panels) the merged MODIS-Aqua-Terra composites.

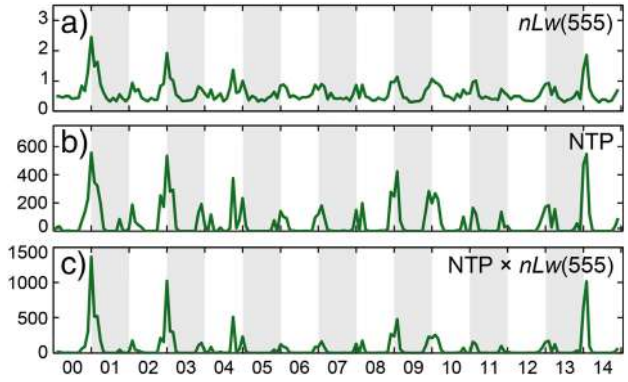

Fig. 3. Temporal evolution of (a) the monthly averaged of *nLw*(555), (b) the number of turbid pixels (NTP) and (c) *nLw*(555) × NTP (c).

non-winter periods in monthly average calculations. As the general patterns of the three monthly time series presented in Fig. 3 are similar, the monthly *nLw(555)* averages were chosen to better quantify the temporal variation of the Douro turbid river plume.

2.2. River discharge, wind and precipitation rate

Daily mean Douro River outflow data, at the Crestuma-Lever dam (D in Fig. 1), were obtained from the SNIRH database (www.snirh.pt).

Wind data were retrieved from NOAA's National Operational Model Archive and Distribution System (NOMADS), which is maintained at NOAA's National Climatic Data Center (NCDC) (Saha et al., 2010). The Climate Forecast System Reanalysis (CFSR) database (http://rda.ucar.edu/pub/cfsr.html) was used, which was developed by NOAA's National Centers for Environmental Prediction (NCEP). The CFSR provides a spatial resolution of 0.5° × 0.5° and a 6-hourly time resolution from January 1979 to December 2014, covering the atmosphere, ocean, sea ice and land. The *u* and *v* wind components (scaled to a reference height of 10 m) were monthly averaged for the research study (41°N, −9.5°E, W in Fig. 1). A previous research carried out along the Iberian Peninsula coast has proved that CFSR data are accurate when compared with in situ buoy measurements (Álvarez et al., 2014).

Monthly precipitation data were retrieved from NOAA/OAR/ESRL PSD, Boulder, Colorado, USA (http://www.esrl.noaa.gov/psd/). This global dataset has been constructed on a 2.5° latitude-longitude grid from 1979 to present day by merging hydrometric gauge observations, estimates inferred from a variety of satellite observations, and the NCEP-NCAR reanalysis. The CPC Merged Analysis of Precipitation (CMAP) dataset was used with success to investigate the annual and interannual variability in large-scale precipitation, showing a reasonable agreement with long-term means (Xie and Arkin, 1997). Data were processed and monthly averaged for the closest available site near the Douro Estuary (R in Fig. 1).

2.3. Climate indices

Monthly NAO and EA teleconnection indices were obtained from the Climate Prediction Center (CPC) at the National Center of Environmental Prediction (NCEP; www.cpc.noaa.gov) over the period 2000–2014. The NAO consists of a north–south dipole of geopotential anomalies, with one center located over Greenland and the other one spanning the region between 35° and 40°N in the central North Atlantic, near the Azores archipelago. EA consists of a north–south dipole that spans the entire North Atlantic Ocean. EA dipole is displaced southeastward the NAO with the centers near 55° N, 20°–35° W and 25°–35° N, 0°–10°W. A detailed description of these indices can be found at http://www.cpc.noaa.gov/data/teledoc/telecontents.shtml.

3. Results and discussion

3.1. Seasonal evaluation

The comparison between monthly averaged series of *nLw(555)*, river discharge and precipitation rate for the period 2000–2014 is shown in Fig. 4a, c. *nLw(555)* data are the average of values within a box close to river mouth (dashed line in Fig. 1 – 41.02°–41.25°N; 9.25°–8.69°W), where the Douro estuarine outflow has more influence on turbidity patterns. A relation between *nLw(555)*, river discharge and precipitation is noticeable (Fig. 4a, c). Correlation coefficient between the Douro River discharge and *nLw(555)* is 0.81 with $p < 0.01$. All maximum peaks of discharge match with *nLw(555)* ones, which indicates the use of high-resolution *nLw(555)* composites as reliable to study the Douro River plume variability at interannual scale (Mendes et al., 2014). For example, the maximum peak of *nLw(555)* is observed during 2000–01, when it was observed the maximum of the Douro River mean daily outflow (>8000 $m^3\ s^{-1}$) (Marta-Almeida et al., 2002; Ruiz Villarreal et al., 2005). A similar correlation is observed in terms of annual climatology with very low values of monthly river inflow during summer months and higher in winter (Fig. 4b). The turbidity is more sensitive to the river discharge in early winter, possibly due to higher sediments supply after summer, which are then carried by river to the coast.

The correlation coefficient between precipitation and *nLw(555)* time series is smaller ($r = 0.58$; $p < 0.01$) (Fig. 4c). However, the maxima correlation was found with a 1-month lag ahead ($r = 0.65$; $p < 0.01$), which confirms the visual analysis from the annual climatological data (Fig. 4d). The precipitation is higher during autumn than during winter. The non-coincident pattern between precipitation and river discharge can be caused by the outflow regulation by several dams along the river's course.

Two typical patterns are observed regarding wind condition during these 15 years (Fig. 4e): Northerly and positive zonal winds are persistent during summer, inducing strong upwelling events (Álvarez et al., 2010, 2011; Fiúza et al., 1998; Fraga, 1981) (Fig. 4e, f); During winter, upwelling-favorable winds are no longer prevalent. Strong southwesterly winds during winter (Fig. 4e, f) are linked to precipitation episodes (Lorenzo et al., 2008; Trigo and DaCamara, 2000), which, in turn, are associated with the highest peaks in river discharge (2000–01, 2002–03, and 2013–14 events) (Fig. 4a, e).

3.2. Wind and river runoff influence on interannual nLw(555) anomalies

The long term (2000–2014) spatio-temporal variability of the Douro turbid plume was characterized by means of longitudinal monthly anomalies of *nLw(555)* averaged for a latitude band coincident with the estuary mouth (41.14° - Fig. 5a). Monthly anomalies of river discharge and meridional and zonal wind components are also represented in Fig. 5b, c, and d, respectively, to further clarify their relationship with anomalous plume patterns. Aqua satellite was launched in July 2002, which partially explains the blank areas observed in 2000 and 2001 (in particular in the winter of 2000/01) – *nLw(555)* composites before July 2002 correspond to MODIS-Terra only (Fig. 5a).

Anomalous high *nLw(555)* values are observed during 2000–01, 2002–03, and 2013–14 winters, while 2001–02, 2004–05, 2005–06, 2007–08, and 2011–12 winters appear to be less impacted by the river discharge and, consequently, by the turbid river plume (Fig. 5a). Relation between river outflow and *nLw(555)* is less important in terms of the turbid plume extent. The wind forcing presents a secondary role, in comparison with river discharge, on the cross-shore propagation of the Douro estuarine plume (Mendes et al., 2014).

Alongshore winds play a key role on the plume confinement and offshore expansion events at interannual scale during positive anomalies of river discharge. This might be part of the explanation to the maximum plume extent found on winter 2002–03 (Fig. 5a), but higher

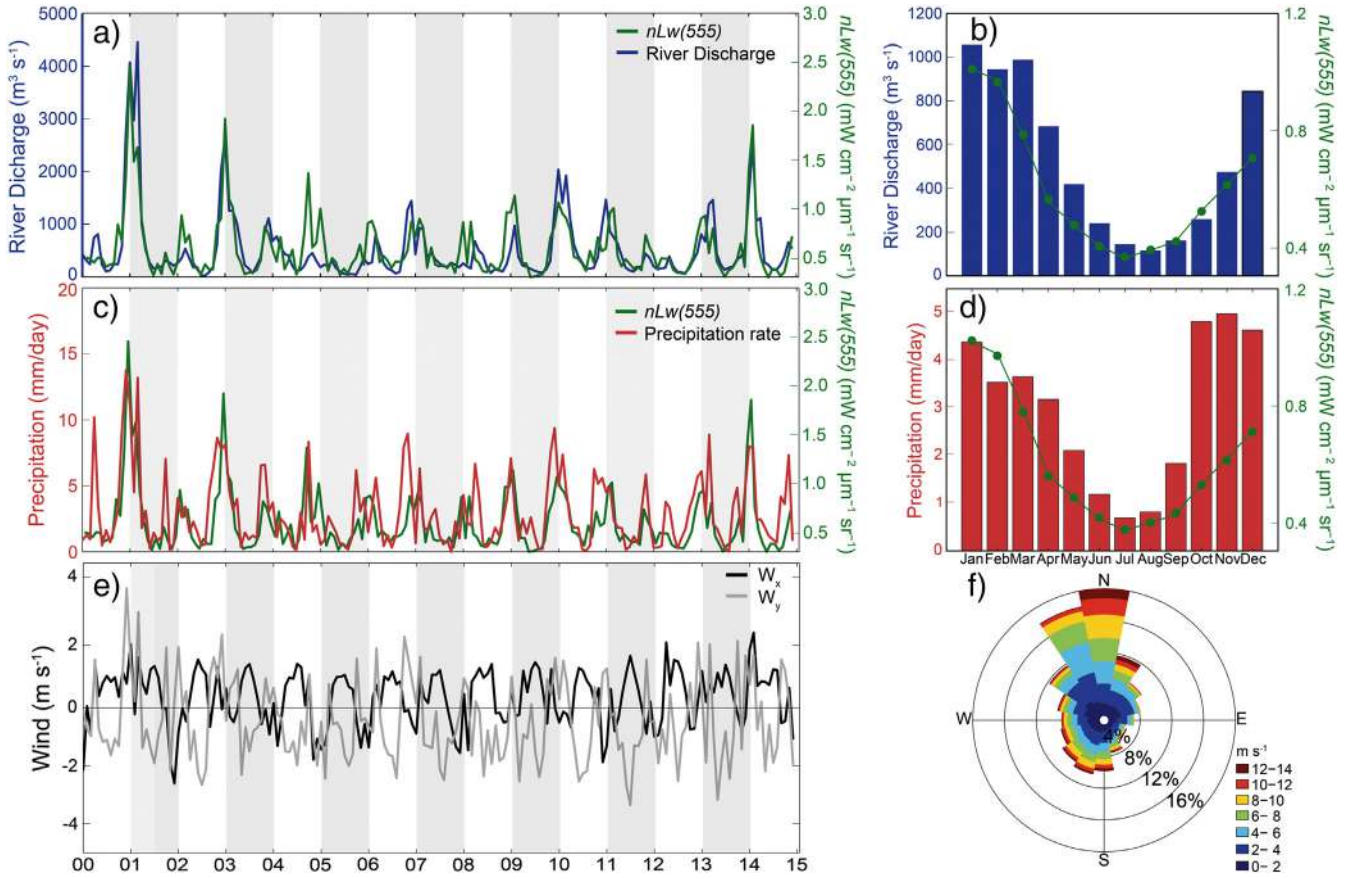

Fig. 4. Temporal evolution (left panels) and mean annual cycles (right panels) of monthly river discharge (a, b) and precipitation. (c, d) with *nLw(555)* data. Monthly average time series of meridional (v) and zonal (u) wind components and wind rose diagram for 2000–2014 period (f).

river discharges and *nLw(555)* anomalies were found on 2000–01 winter (Fig. 4a). Downwelling-favorable winds during winter 2000–01 were stronger than during 2002–03, which tend to confine the plume to the coast and consequently reduce its offshore transport (Mendes et al., 2014; Otero et al., 2008).

Northerly winds induce winter upwelling events which have similar characteristics to those observed during summer, when precipitation and river discharge are minimum. Large negative *nLw(555)* anomalies are usually associated with winters with low river discharge and precipitation rate, which in turn is associated with a predominance of upwelling-favorable winds, i.e. winters of 2001–02, 2004–05, 2005–06, 2007–08, and 2011–12 (Fig. 5a, c, d).

3.3. Seasonal and interannual spatial patterns

Apart from the known correlation between wind and precipitation in the Douro basin and consequently on the variation of the freshwater discharge, wind also affects the plume propagation patterns along the coast. In the previous section, it was shown that wind impacts the offshore extension of the plume, decreasing its dependence on river discharge changes.

The seasonal and interannual variation of the Douro estuarine plume is studied, in terms of spatial differences, calculating the *nLw(555)* maxima over the 15 years of data in every pixel of the study region. The results are depicted as a function of months and years (Fig. 6a, b). The contours of the plume area in different months and years, following the 1.1 mW cm^{-2} μm^{-1} sr^{-1} criterion (Mendes et al., 2014), are shown in Fig. 6c, d). Months without significant river discharges events are not depicted in Fig. 6c for the sake of clarity. Following the same principle, Fig. 6d shows the average of the plume area only for 3 years with significant positive (2001, 2003, and 2014) and negative river discharge anomalies (2002, 2006, and 2012).

The *nLw(555)* maxima near the coast was found in winter months (December, January and February) as expected (Fig. 6a). However, observing both Fig. 6a, b is found a significant *nLw(555)* maxima at southwest of the Douro river mouth, during October 2004. For the open ocean, peak nLw(555) values occurred in April and May due to the increase of sunlight radiation, which stimulates phytoplankton blooms (changing water turbidity). Nevertheless, the typical values found in those regions (0.6–1 mW cm^{-2} μm^{-1} sr^{-1}) are considerable lower than for near shore regions (>1 mW cm^{-2} μm^{-1} sr^{-1}) where the influence of the Douro plume is higher. The typical offshore extent of the Douro turbid plume is also inferred from Fig. 6a. The 9.5°W longitudinal boundary (about 50–60 km from coast) can be considered as the distinguished limit of riverine turbidity. The limit of the continental shelf in this region is around 9.5°W, e.g. this bathymetric constraint (Fig. 1) also influences and blocks the seaward excursion of the buoyant turbid plume propagation as established by Lee and Valle-Levinson (2012). According to the statistics results shown in Fig. 6a, the largest percentage of *nLw(555)* maxima in the four seasons decreases in the following order: winter > spring > autumn > summer. The area of *nLw(555)* maxima for winter was approximately 47.7% of the total area represented and similar during spring (47.5%), mostly corresponding to open sea regions where the biological activity is important during spring. For autumn, this area is about 4.7%, mostly related with the October 2004 event. In summer this area is nearly null (<0.1%). The analysis of the monthly averaged plume area and its seaward extension (Fig. 6c) shows an expected agreement with mean annual cycles of monthly *nLw(555)* data (Fig. 4b). Plume area and offshore extension are larger (in average) during January and February, followed by other related winter and/or rainy months as March, November and December. Turbid

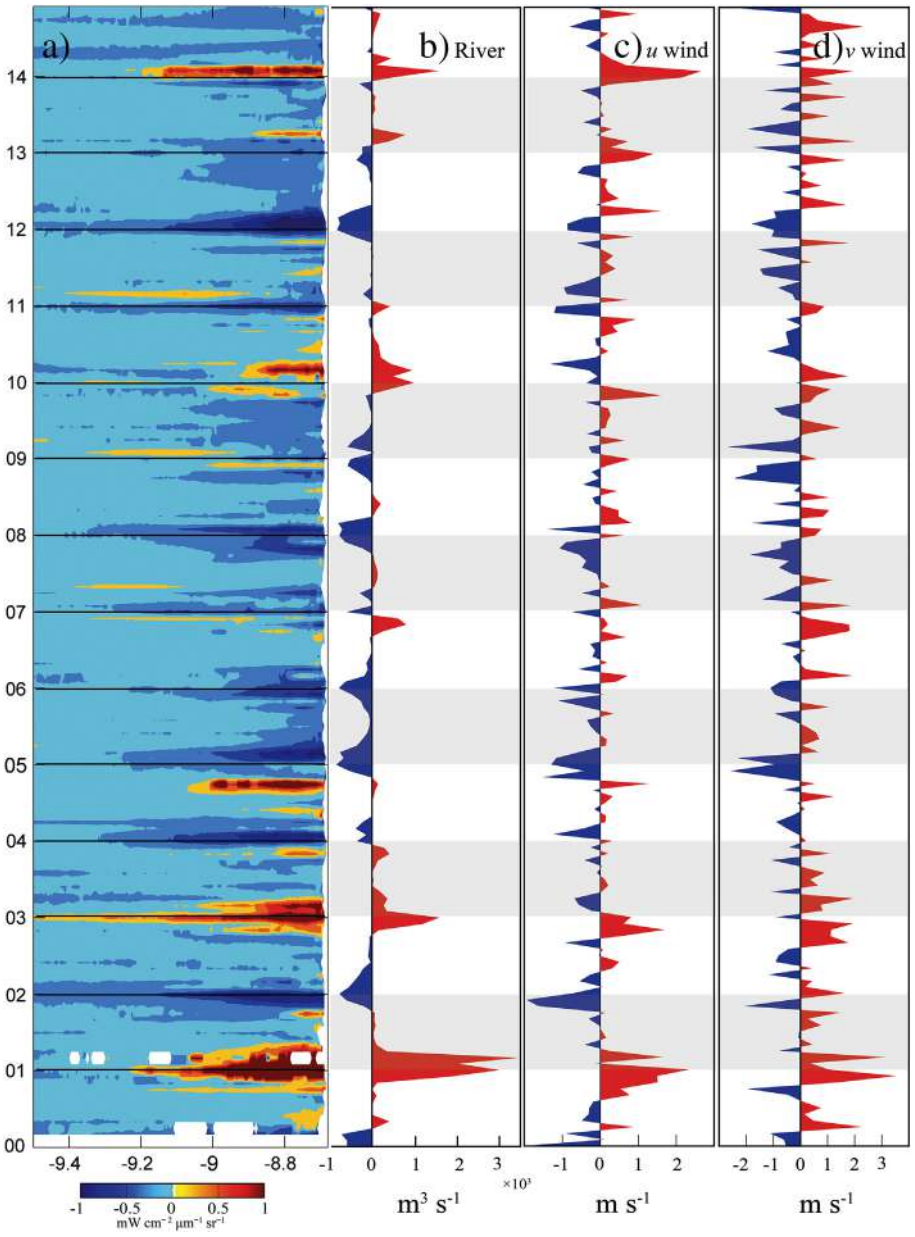

Fig. 5. (a) Hovmöller diagram of monthly *nLw(555)* anomalies for a latitudinal band coincident with Douro River mouth. (b) Douro river discharge and (c) zonal and (d) meridional wind monthly anomalies. (For interpretation of the references to color in this figure, the reader is referred to the web version of this article.)

plume events are rare in April and October and almost non-existent between May and September (Fig. 6c).

The largest plume events in winter are clearly distinguishable and represent three different spatial characteristics (see Figs. 5, 6a and b). The *nLw(555)* value for the winter of 2000–2001 is represented in a large area located north of the Douro River mouth (orange in Fig. 5b). Fig. 6d also reveals that the plume event found in 2001 had a higher impact on the northern region. This synoptic pattern observed is typical of the plume propagation affected by strong southerly and southwesterly winds (Mendes et al., 2014) The large plume seaward extension (about 50 km) found during January of 2003 (Fig. 5a) is represented in Fig. 6b by yellow-green color in the open-sea region. The high river discharge event of January of 2003 was characterized by weak winds in the study region. In this case the plume propagation is mostly controlled by the estuarine discharge, and its offshore extension off the estuary mouth is similar to that found for the 2001 event (Fig. 6d), despite the difference in river inflow between both events (Fig. 4a). In January 2014, strong westerly wind conditions were observed, confining the plume to the coast and producing a continuous alongshore turbid band northward (Mendes et al., 2014). This pattern is depicted by the dark-pink color in Fig. 6b corresponding to 2014. The offshore plume extension both south and north of the estuary mouth is equivalent (Fig. 6d), indicating the westerly wind impact on the plume propagation.

3.4. Relation of atmospheric indices with the turbid plume

The correlation between variables presented in Fig. 4 (*nLw(555)*, river discharge, and precipitation rate) and the teleconnection indices (NAO and EA) were calculated for winter months (DJF) from 2000 to 2014. In addition, time lags between the variables were also considered: Lag 1 represents JFM values of *nLw(555)*, Douro River discharger and precipitation rate; Lag 2 corresponds to FMA and so on. The correlation coefficients between DJF atmospheric patterns and the referred variables (with different lags) are depicted in Fig. 7.

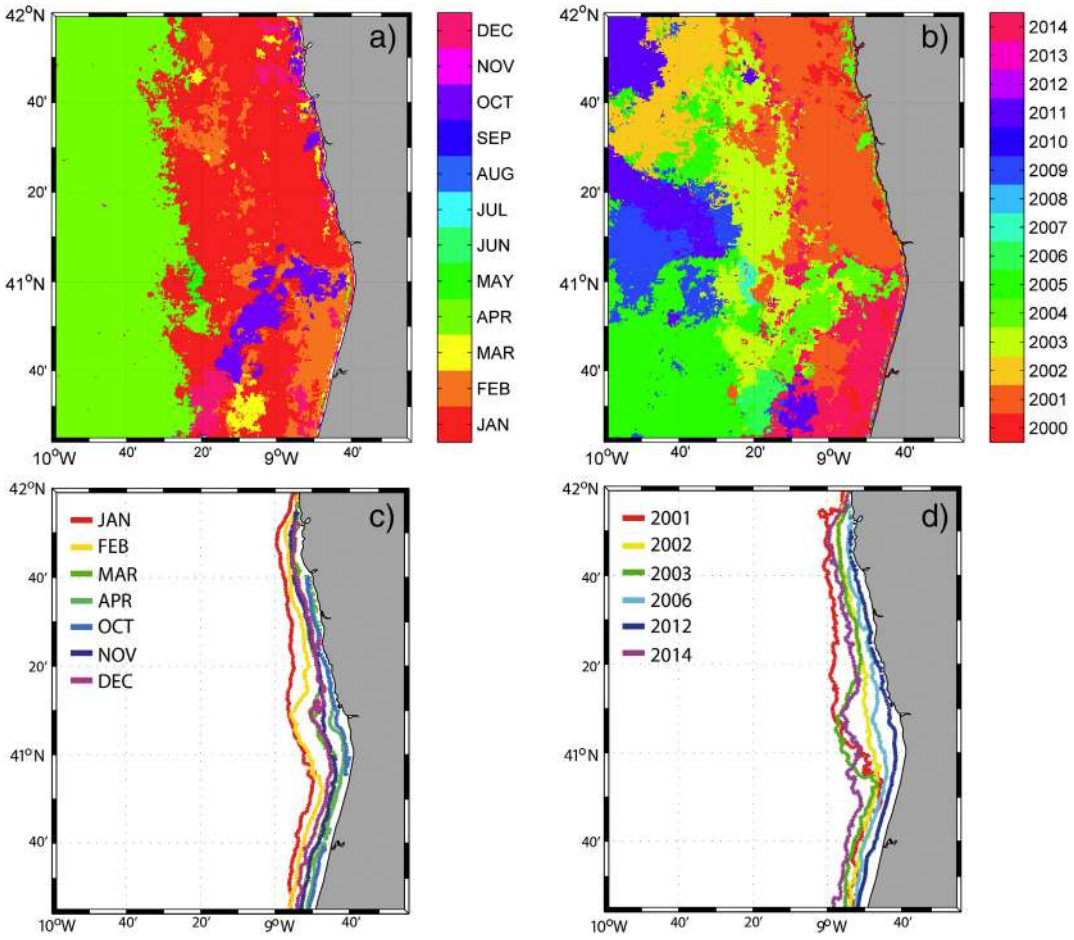

Fig. 6. Spatial-temporal distribution of the timing of *nLw(555)* maxima in terms of months (a) and years (b) from 2000 to 2014. Contours of plume limits from monthly and yearly average following Mendes et al. (2014) criterion. (For interpretation of the references to color in this figure, the reader is referred to the web version of this article.)

The EA index shows to be directly correlated with the three variables. A positive EA pattern is related to periods of predominant low pressure in the study area during winter. Under this situation, more cold fronts reach the Northwestern Iberian coast resulting in increased precipitation (deCastro et al., 2006a, b; Lorenzo and Taboada, 2005). Precipitation has a significant correlation with EA index ($r = 0.64$) when no lag is considered. Then, this correlation coefficient decreases continuously until no significant values are observed with lags of 2, 3, and 4 months (Fig. 7). This result is in line with a previous study carried out by Lorenzo and Taboada (2005), in the southern part of Galicia and in the Atlantic coast (about 80 km north of the Douro estuary). Regarding the EA influence on river discharge, significant correlations were found for all lags ($r > 0.46$) with a maximum ($r = 0.54$) when 1-month lag is considered. This result agrees with the study of deCastro et al. (2006a, b) for the Minho River (Fig. 1). They found smaller correlation coefficients between the Minho River discharge and EA index with 0- and 1-month lag (close to 0.40). Significant correlation coefficients were observed between EA index and *nLw(555)* for all lags with a maximum ($r = 0.51$) for a 1-month lag. The influence of EA index could be related with the prevalence of southerly winds over the shelf, which tend to maximize the turbid signal near the river mouth (deCastro et al., 2008a, b; Mendes et al., 2014).

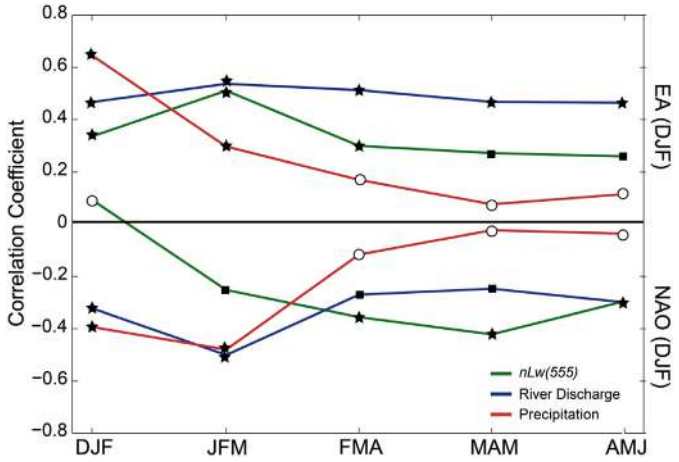

Fig. 7. DJF atmospheric correlation patterns (EA – above; NAO – below) with *nLw(555)*, river flow, and precipitation from 2000 to 2014. A 0 lag corresponds to the DJF period, 1 to JFM period, and so on. Results with a significance level >95% are represented by stars, >90% by squares, and <90% by empty circles.

The correlation coefficient between river flow and the NAO index reaches its maximum value of −0.50 for a time lag of 1 month. This result is in the same line with those obtained by Trigo et al. (2004) for Atlantic Iberian rivers, including the Douro River. Nevertheless, it is smaller than the one found by these authors from 1978 to 1998 ($r = -0.76$) and smaller than the one obtained for the Minho River by deCastro et al. (2006a, b) ($r = -0.54$) from 1970 to 2005. This contrasts with the tendency for correlations to diminish from south to north over the region (deCastro et al., 2006a, b; Trigo et al., 2004). However, deCastro et al. (2006a, b) also found that correlation for the Minho River decreases in time, reaching values below −0.4 for periods from 1980 to 2005. The correlation coefficients obtained between precipitation anomaly and NAO index show a similar pattern to correlation between the river discharge anomaly and NAO. Maximum correlation is

found at 1-month lag ($r = -0.48$) and drops to insignificant values for subsequent lags (Fig. 7).

The correlation between *nLw(555)* anomalies and NAO index shows unexpected results (Fig. 7). A significant maximum correlation of −0.42 is reached for a time lag of 3 months, corresponding to early spring months (MAM). Several physical and biogeochemical processes can change ocean water turbidity, obscuring the relation between plume-related turbidity and atmospheric patterns. This correlation could be explained in terms of biological influence (i.e. coastal blooms) during spring upwelling events (3-month lags).

March and April *nLw(555)* composites after a positive and negative DJF NAO phase are depicted in Fig. 8a, b, respectively. Under a positive DJF NAO (Fig. 8a), turbid values during the subsequent spring are lower than after a negative DJF NAO (Fig. 8b). The main differences were found along the coast, near the river mouth. Medium turbid values (0.6–1 mW cm^{-2} μm^{-1} sr^{-1}) are confined to a short coastal band of about 10 km after a positive DJF NAO (Fig. 8a) and up to 30 km offshore after a negative one (Fig. 8b). Phytoplankton blooms are usually a source of medium turbid values (0.6–1 mW cm^{-2} μm^{-1} sr^{-1}) on coastal waters, but significantly smaller compared with the turbidity induced by mid-latitude river outflows (e.g. Saldías et al., 2016b).

The positive phase of the NAO (JFM) is characterized by colder, drier winters and by stronger northerly winds, which favor winter upwelling events in the Douro coastal region (deCastro et al., 2006a, b; Lorenzo and Taboada, 2005, deCastro et al., 2008a, b). An increase of northerly winds, together with a decrease of sea surface temperature and atmospheric conditions, inhibit water-column stratification and, combined with lower nutrient availability, appears to limit the phytoplankton development (Barton et al., 2003). Thus, it is reasonable to assume that this higher correlation between NAO and *nLw(555)* at 3-month lag is due to the upwelling season shift towards winter, which can affect the magnitude and the timing of coastal spring blooms off the Douro River.

3.5. The anomalous 2004 event

An anomalous turbid patch (values above 3–4 mW cm^{-2} μm^{-1} sr^{-1}) was repeatedly observed in daily *nLw(555)* images during autumn 2004 (Figs. 4a and 5a). The evolution of this anomalous event are presented in Fig. 9. These images show a patch with very high *nLw(555)* values unconnected with the Douro River discharge. The turbid feature development starts south of Douro estuary (between the Douro estuary mouth and the Ria de Aveiro) at about 15 km offshore on 25 September (Fig. 9), presenting several ramifications but none of them suggesting a fluvial origin (26 and 27 September, Fig. 10). The bloom increases rapidly both in area and in magnitude after 28 September, when *nLw(555)* reaches values of about 4 mW cm^{-2} μm^{-1} sr^{-1}. Well-developed patterns related to freshwater plume turbidity are unexpected when river discharge is below 500 m^3 s^{-1} (Mendes et al., 2014; Teodoro et al., 2009). The daily river discharge between the end of September and the beginning of October is low (~300 m^3 s^{-1}), although over the average for September/October (Fig. 4a, b). Spectra of normalized water leaving radiance taken from the bloom core maximum from all available daily images between 28 September and 12 October are depicted in Fig. 10. At the beginning of this period, after 15 days of upwelling-favorable winds, maxima turbid values are observed in bands near 550 nm (*nLw(547)* = 3.9 mW cm^{-2} μm^{-1} sr^{-1}; *nLw(555)* = 3.8 mW cm^{-2} μm^{-1} sr^{-1}, Figs. 9 and 10). The intensity of the water leaving radiance tends to increase in all bands in time, with a maximum of 8.1 and 7.6 mW cm^{-2} μm^{-1} sr^{-1} for *nLw(547)* and *nLw(555)*, respectively. The spectra pattern remains unchanged until 7 October. Afterwards, those turbid features merged into a larger and brighter bloom with *nLw(555)* values around 5 mW cm^{-2} μm^{-1} sr^{-1} (11 and 12 October, Fig. 9). On these dates, the bloom core spectrum is characterized by a peak at 488 nm (7.0 and 5.6 mW cm^{-2} μm^{-1} sr^{-1}, Fig. 10) with higher reflectance in the blue region, but with a *nLw(555)* value higher for the first case (Fig. 10). Unfortunately, the valid MODIS data between 8 and 10 October is insufficient to properly examine the bloom evolution between those contrasting spectra patterns (Fig. 10).

A biological factor may be responsible or co-responsible for these very high turbid values. One of the best assumption is a coccolithophore bloom, which usually causes a very bright patch of water with a turquoise color (IOCCG, 2014; Moore et al., 2012). These blooms can be visible in ocean color images as a result of light scattering by the coccolith plates detached from cells (from death or overproduction) suspended in near-surface waters (Moore et al., 2009). The transition from upwelling to downwelling (Summer-Autumn) is often reported to be the most favorable time for coccolithophore growth (Giraudeau et al., 1993; Ziveri et al., 1995). This transition is typically observed off the NW Iberian Peninsula during October (Figueiras et al., 2002) and is characterized by intermittent upwelling events, as in Fig. 9. These conditions promote the confluence of warmer oceanic waters into colder and nutrient rich coastal upwelled waters (Moita et al., 2010; Silva et al., 2009).

Coccolithophore blooms and turbid plumes are usually discriminated by the wavelength peak for reflected light, which is around 555 nm for sediment-dominated waters and 490 nm for coccolithophore

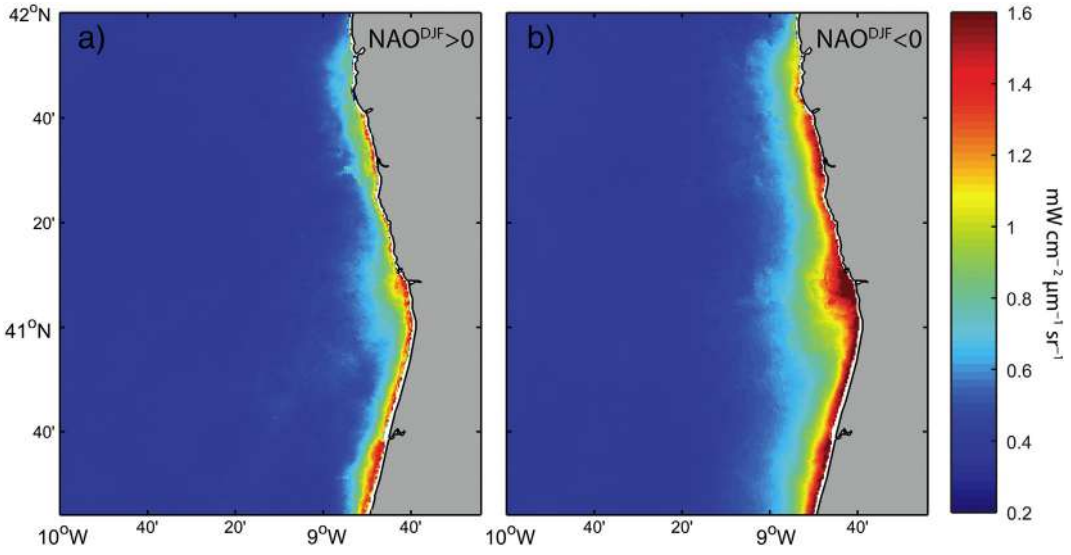

Fig. 8. *nLw(555)* spring composites (March and April) after a (a) positive and (b) negative NAO winter phase (DJF).

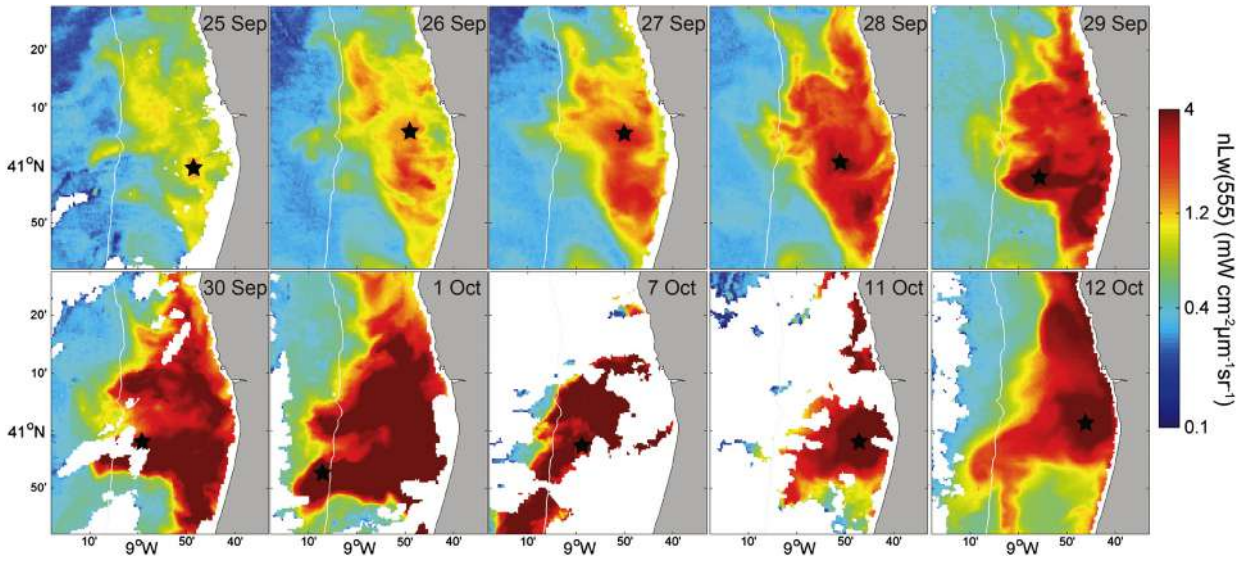

Fig. 9. *nLw(555)* daily available images from 26 September to 12 October of 2004.

bloom (IOCCG, 2014; Moore et al., 2012). That is the spectrum shape of 11 and 12 October, indicating that this higher *nLw(555)* anomaly (Fig. 4a) could be induced by a coccolithophore bloom (Fig. 10). A conclusion from the spectrum analysis between 25 September and 7 October is still pending. Nevertheless, the coastal detection of any coccolithophore bloom will be certainly affected by the background optical properties of the water during the event. For example, the presence of detritus and colored dissolved matter can attenuate the reflectance in the blue region, causing a peak shift towards 555 nm, as already reported for a bloom event in the English Channel (Gordon et al., 2009; Moore et al., 2012; Smyth et al., 2002).

The real source of these anomalous turbid features during autumn 2004 remains unclear. The detection of coccolithophore blooms apart from other phenomena related to bright water by remote sensing is a challenging task. The lack of available in situ data for this period makes our analysis inconclusive. However, this phenomenon could give a reasonable explanation of disagreements between the Douro River discharge and *nLw(555)* time series for this single case. Despite these limitations, *nLw(555)* MODIS imagery can be a useful tool, in combination with satellite imagery of particulate inorganic carbon (PIC) concentration, to explore other turbid anomalies that can be related to phytoplankton blooms at higher temporal resolution in the Northwestern Iberian Peninsula.

4. Conclusions

The seasonal and interannual variability of the Douro turbid plume was evaluated considering the river discharge, wind, precipitation rates and climate patterns, namely NAO and EA indices. The main conclusions of this research can be summarized as:

- High correlations were obtained between monthly time series of *nLw(555)*, river discharge and precipitation rates. Anomalous positive turbid plume events were observed in 2000–01, 2002–03 and 2013–14 winters, while negative anomalies were identified in 2001–02, 2004–05, 2005–06, 2007–08 and 2011–12 winters. All peak values of *nLw(555)* matched with extreme local forcing. The autumn of 2004 is a remarkable exception.
- Positive *nLw(555)* anomalies are often related with south and westerly winds that favors precipitation and, consequently, increases monthly river discharge. Although strong downwelling-favorable winds usually enhance the positive anomaly signal, it also reduces the turbid plume width. Negative anomalies are usually associated with the predominance of upwelling-favorable winds in winter when precipitation and river discharge are minimum.
- The EA pattern plays a key role on precipitation rate in the Douro estuary region, being directly correlated with all variables and in agreement with previous studies. The correlation patterns between *nLw(555)* and DJF EA index present a peak at 1-month lag ($r = 0.51$), as well as with the river discharge ($r = 0.54$).
- The correlation coefficient between DJF NAO index and Douro river discharge is high (-0.50), for a time lag of 1-month. Correlations between *nLw(555)* and DJF NAO index present a peak of -0.42 at 3-month lag. The spring correlation (MAM) is possibly affected by upwelling season shifts, affecting biological coastal production.
- An extreme anomalous turbid pattern not related to estuarine outflow was found south of the Douro river mouth during the autumn of 2004. Despite the real source of this event remains uncertain, a coccolithophore bloom could be the most reasonable explanation.

Acknowledgments

The first author has been supported by the Portuguese Science Foundation through a doctoral grant (SFRH/BD/79555/2011). NV is supported by a post-doctoral grant (SFRH/BPD/110615/2015). GS has been supported by a Fulbright-Becas Chile scholarship during the initial state of this manuscript. This study was supported by the National Foundation for Science and Technology – FCT, through CESAM (UID/AMB/50017/2013), Xunta de Galicia under the project Programa de Consolidación e Estruturación de Unidades de Investigación (Grupos

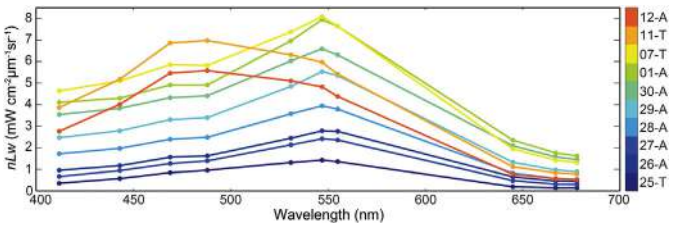

Fig. 10. *nLw* spectra from the pixels marked with a black star on daily images of Fig. 9 from Aqua (A) or Terra (T) satellite.

de Referencia Competitiva) funded by European Regional Development Fund (FEDER) and under the project EM2013/003.

References

Álvarez, I., Ospina-Alvarez, N., Pazos, Y., deCastro, M., Bernardez, P., Campos, M.J., Gomez-Gesteira, J.L., Alvarez-Ossorio, M.T., Varela, M., Gomez-Gesteira, M., Prego, R., 2009. A winter upwelling event in the Northern Galician Rias: frequency and oceanographic implications. Estuar. Coast. Shelf Sci. 82:573–582. http://dx.doi.org/10.1016/j.ecss.2009.02.023.

Álvarez, I., Gomez-Gesteira, M., deCastro, M., Gomez-Gesteira, J.L., Dias, J.M., 2010. Summer upwelling frequency along the western Cantabrian coast from 1967 to 2007. J. Mar. Syst. 79:218–226. http://dx.doi.org/10.1016/j.jmarsys.2009.09.004.

Álvarez, I., Gomez-Gesteira, M., deCastro, M., Lorenzo, M.N., Crespo, A.J.C., Dias, J.M., 2011. Comparative analysis of upwelling influence between the western and northern coast of the Iberian Peninsula. Cont. Shelf Res. 31:388–399. http://dx.doi.org/10.1016/j.csr.2010.07.009.

Álvarez, I., Gomez-Gesteira, M., deCastro, M., Carvalho, D., 2014. Comparison of different wind products and buoy wind data with seasonality and interannual climate variability in the southern Bay of Biscay (2000–2009). Deep-Sea Res. II Top. Stud. Oceanogr. 106:38–48. http://dx.doi.org/10.1016/j.dsr2.2013.09.028.

Aurin, D., Mannino, A., Franz, B., 2013. Spatially resolving ocean color and sediment dispersion in river plumes, coastal systems, and continental shelf waters. Remote Sens. Environ. 137:212–225. http://dx.doi.org/10.1016/j.rse.2013.06.018.

Azevedo, I.C., Duarte, P.M., Bordalo, A.A., 2008. Understanding spatial and temporal dynamics of key environmental characteristics in a mesotidal Atlantic estuary (Douro, NW Portugal). Estuar. Coast. Shelf Sci. 76:620–633. http://dx.doi.org/10.1016/j.ecss.2007.07.034.

Azevedo, I.C., Bordalo, A.A., Duarte, P.M., 2010. Influence of river discharge patterns on the hydrodynamics and potential contaminant dispersion in the Douro estuary (Portugal). Water Res. 44:3133–3146. http://dx.doi.org/10.1016/j.watres.2010.03.011.

Baith, K., Lindsay, R., Fu, G., McClain, C.R., 2001. Data analysis system developed for ocean color satellite sensors. EOS Trans. Am. Geophys. Union 82:202. http://dx.doi.org/10.1029/01EO00109.

Barton, A., Greene, C., Monger, B., Pershing, A., 2003. The continuous plankton recorder survey and the North Atlantic oscillation: interannual- to multidecadal-scale patterns of phytoplankton variability in the North Atlantic Ocean. Prog. Oceanogr. 58:337–358. http://dx.doi.org/10.1016/j.pocean.2003.08.012.

Binding, C.E., Bowers, D.G., 2003. Measuring the salinity of the Clyde Sea from remotely sensed ocean colour. Estuar. Coast. Shelf Sci. 57:605–611. http://dx.doi.org/10.1016/S0272-7714(02)00399-2.

Burrage, D., Wesson, J., Martinez, C., Pérez, T., Möller, O., Piola, A., 2008. Patos Lagoon outflow within the Río de la Plata plume using an airborne salinity mapper: Observing an embedded plume. Cont. Shelf Res. 28:1625–1638. http://dx.doi.org/10.1016/j.csr.2007.02.014.

deCastro, M., Lorenzo, N., Taboada, J., Sarmiento, M., Alvarez, I., Gomez-Gesteira, M., 2006a. Influence of teleconnection patterns on precipitation variability and on river flow regimes in the Miño River basin (NW Iberian Peninsula). Clim. Res. 32:63–73. http://dx.doi.org/10.3354/cr032063.

deCastro, M., Alvarez, I., Varela, M., Prego, R., Gómez-Gesteira, M., 2006b. Miño River dams discharge on neighbor Galician Rias Baixas (NW Iberian Peninsula): Hydrological, chemical and biological changes in water column. Estuar. Coast. Shelf Sci. 70:52–62. http://dx.doi.org/10.1016/j.ecss.2006.05.035.

deCastro, M., Gómez-Gesteira, M., MN, L., Alvarez, I., 2008a. Influence of atmospheric modes on coastal upwelling along the western coast of the Iberian Peninsula, 1985 to 2005. Clim. Res. 36, 169–179.

deCastro, M., Gómez-Gesteira, M., Alvarez, I., Lorenzo, M., Cabanas, J.M., Prego, R., Crespo, A.J.C., 2008b. Characterization of fall–winter upwelling recurrence along the Galician western coast (NW Spain) from 2000 to 2005: dependence on atmospheric forcing. J. Mar. Syst. 72:145–158. http://dx.doi.org/10.1016/j.jmarsys.2007.04.005.

Chícharo, M.A., Esteves, E., Santos, A.M.P., Dos Santos, A., Peliz, Á., Ré, P., 2003. Are sardine larvae caught off northern Portugal in winter starving? An approach examining nutritional conditions. Mar. Ecol. Prog. Ser. 257:303–309. http://dx.doi.org/10.3354/meps257303.

Dias, J.M.A., 1987. Dinâmica sedimentar e evolução recente da plataforma continental portuguesa setentrional. University of Lisbon, Lisbon, Portugal.

Dias, J.M.A., 1990. A Evolução Actual do Litoral Português. Protecção Civ. III. pp. 2–15.

Dyer, K.R., 1973. Estuaries: A Physical Introduction, Estuarine and Coastal Marine Science. John Wiley & Sons, Inc. http://dx.doi.org/10.1016/0302-3524(73)90042-X.

Dzwonkowski, B., Yan, X.H., 2005. Tracking of a Chesapeake Bay estuarine outflow plume with satellite-based ocean color data. Cont. Shelf Res. 25:1942–1958. http://dx.doi.org/10.1016/j.csr.2005.06.011.

Esteban-Parra, M.J., Rodrigo, F.S., Castro-Diez, Y., 1998. Spatial and temporal patterns of precipitation in Spain for the period 1880–1992. Int. J. Climatol. 18:1557–1574. http://dx.doi.org/10.1002/(SICI)1097-0088(19981130)18:14<1557::AID-JOC328>3.3.CO;2-A.

Fernández-Nóvoa, D., Mendes, R., deCastro, M., Dias, J.M., Sánchez-Arcilla, A., Gómez-Gesteira, M., 2015. Analysis of the influence of river discharge and wind on the Ebro turbid plume using MODIS-Aqua and MODIS-Terra data. J. Mar. Syst. 142:40–46. http://dx.doi.org/10.1016/j.jmarsys.2014.09.009.

Figueiras, F.G., Labarta, U., Fernández Reiriz, M.J., 2002. Coastal upwelling, primary production and mussel growth in the Rías Baixas of Galicia. Hydrobiologia 484:121–131. http://dx.doi.org/10.1023/A:1021309222459.

Fiúza, A.F.G., Hamann, M., Ambar, I., Díaz Del Río, G., González, N., Cabanas, J.M., 1998. Water masses and their circulation off western Iberia during May 1993. Deep. Res. Part I Oceanogr. Res. Pap. 45:1127–1160. http://dx.doi.org/10.1016/S0967-0637(98)00008-9.

Fong, D.A., Geyer, W.R., 2001. Response of a river plume during an upwelling favorable wind event. J. Geophys. Res. http://dx.doi.org/10.1029/2000JC900134.

Fraga, F., 1981. Upwelling off the Galacian Coast, northwest Spain. In: Richardson, F.A. (Ed.), Coastal Upwelling. American Geophysical Union, Washington D.C.: pp. 176–182 http://dx.doi.org/10.1029/CO001p0176.

Franz, B.A., Werdell, P.J., Meister, G., Kwiatkowska, E.J., Bailey, S.W., Ahmad, Z., McClain, C.R., 2006. MODIS land bands for ocean remote sensing applications. Proc. Ocean Optics XVIII (Montreal, Canada).

García Berdeal, I., Hickey, B.M., Kawase, M., 2002. Influence of wind stress and ambient flow on a high discharge river plume. J. Geophys. Res. 107:3130. http://dx.doi.org/10.1029/2001JC000932.

Garvine, R.W., 1974. Dynamics of small-scale oceanic fronts. J. Phys. Oceanogr. http://dx.doi.org/10.1175/1520-0485(1974)004<0557:DOSSOF>2.0.CO;2.

Giraudeau, J., Monteiro, P.M.S., Nikodemus, K., 1993. Distribution and malformation of living coccolithophores in the northern Benguela upwelling system off Namibia. Mar. Micropaleontol. 22:93–110. http://dx.doi.org/10.1016/0377-8398(93)90005-I.

Gordon, H.R., Smyth, T.J., Balch, W.M., Boynton, G.C., Tarran, G.A., 2009. Light scattering by coccoliths detached from Emiliania huxleyi. Appl. Opt. 48:6059–6073. http://dx.doi.org/10.1364/AO.48.006059.

Hetland, R.D., 2005. Relating river plume structure to vertical mixing. J. Phys. Oceanogr. 35:1667–1688. http://dx.doi.org/10.1175/JPO2774.1.

Horner-Devine, A.R., Hetland, R.D., MacDonald, D.G., 2015. Mixing and transport in coastal river plumes. Annu. Rev. Fluid Mech. 47:569–594. http://dx.doi.org/10.1146/annurev-fluid-010313-141408.

IOCCG, 2014. Phytoplankton functional types from space. Reports and Monographs of the International Ocean Colour Coordinating Group.

Klemas, V., 2011. Remote Sensing of Sea Surface Salinity: An Overview with Case Studies. J. Coast. Res. 276:830–838. http://dx.doi.org/10.2112/JCOASTRES-D-11-00060.1.

Lee, J., Valle-Levinson, A., 2012. Influence of bathymetry on hydrography and circulation at the region between an estuary mouth and the adjacent continental shelf. Cont. Shelf Res. 41:77–91. http://dx.doi.org/10.1016/j.csr.2012.04.006.

Lorenzo, M.N., Taboada, J.J., 2005. Influences of atmospheric variability on freshwater input in Galician Rías in winter. J. Atmos. Ocean Sci. 10:377–387. http://dx.doi.org/10.1080/17417530601127472.

Lorenzo, M.N., Taboada, J.J., Gimeno, L., 2008. Links between circulation weather types and teleconnection patterns and their influence on precipitation patterns in Galicia (NW Spain). Int. J. Climatol. 28:1493–1505. http://dx.doi.org/10.1002/joc.1646.

Marta-Almeida, M., Dubert, J., Peliz, Á., 2002. Simulations of extreme shelf current Along the North-Western Iberian Shelf forced by wind and river runoff. 3rd Iberian Meeting on Geophysics and Geodesy. Valencia, Spain, pp. 1555–1559.

Mendes, R., Vaz, N., Fernández-Nóvoa, D., da Silva, J.C.B., deCastro, M., Gómez-Gesteira, M., Dias, J.M., 2014. Observation of a turbid plume using MODIS imagery: the case of Douro estuary (Portugal). Remote Sens. Environ. 154:127–138. http://dx.doi.org/10.1016/j.rse.2014.08.003.

Mendes, R., Sousa, M.C., deCastro, M., Gómez-Gesteira, M., Dias, J.M., 2016. New insights on Western Iberian Buoyant Plume: interaction between the Douro and Minho river plumes during winter conditions. Prog. Oceanogr.

Moita, M.T., Silva, A., Palma, S., Vilarinho, M.G., 2010. The coccolithophore summer–autumn assemblage in the upwelling waters of Portugal: patterns of mesoscale distribution (1985–2005). Estuar. Coast. Shelf Sci. 87:411–419. http://dx.doi.org/10.1016/j.ecss.2010.01.025.

Molleri, G.S.F., Novo, E.M.L.D.M., Kampel, M., 2010. Space-time variability of the Amazon River plume based on satellite ocean color. Cont. Shelf Res. 30:342–352. http://dx.doi.org/10.1016/j.csr.2009.11.015.

Moore, T.S., Campbell, J.W., Dowell, M.D., 2009. A class-based approach to characterizing and mapping the uncertainty of the MODIS ocean chlorophyll product. Remote Sens. Environ. 113:2424–2430. http://dx.doi.org/10.1016/j.rse.2009.07.016.

Moore, T.S., Dowell, M.D., Franz, B.a., 2012. Detection of coccolithophore blooms in ocean color satellite imagery: a generalized approach for use with multiple sensors. Remote Sens. Environ. 117:249–263. http://dx.doi.org/10.1016/j.rse.2011.10.001.

Nezlin, N.P., DiGiacomo, P.M., Stein, E.D., Ackerman, D., 2005. Stormwater runoff plumes observed by SeaWiFS radiometer in the Southern California Bight. Remote Sens. Environ. 98:494–510. http://dx.doi.org/10.1016/j.rse.2005.08.008.

Oliveira, I.B.M., Valle, a.J.S.F., Miranda, F.C.C., 1982. Littoral problems in the Portuguese West Coast. Coast. Eng. 3, 1950–1969.

Otero, P., Ruiz-Villarreal, M., Peliz, A., 2008. Variability of river plumes off Northwest Iberia in response to wind events. J. Mar. Syst. 72:238–255. http://dx.doi.org/10.1016/j.jmarsys.2007.05.016.

Otero, P., Ruiz-Villarreal, M., Peliz, A., 2009. River plume fronts off NW Iberia from satellite observations and model data. ICES J. Mar. Sci. 66:1853–1864. http://dx.doi.org/10.1093/icesjms/fsp156.

Palacios, S.L., Peterson, T.D., Kudela, R.M., 2009. Development of synthetic salinity from remote sensing for the Columbia River plume. J. Geophys. Res. Oceans 114 (C00B05). 10.1029/2008JC004895.

Peliz, Á., Rosa, T.L., Santos, A.M.P., Pissarra, J.L., 2002. Fronts, jets, and counter-flows in the Western Iberian upwelling system. J. Mar. Syst. 35:61–77. http://dx.doi.org/10.1016/S0924-7963(02)00076-3.

Picado, A., Alvarez, I., Vaz, N., Varela, R., Gomez-Gesteira, M., Dias, J.M., 2014. Assessment of chlorophyll variability along the northwestern coast of Iberian Peninsula. J. Sea Res. http://dx.doi.org/10.1016/j.seares.2014.01.008.

Piola, A.R., Romero, S.I., Zajaczkovski, U., 2008. Space–time variability of the Plata plume inferred from ocean color. Cont. Shelf Res. 28:1556–1567. http://dx.doi.org/10.1016/j.csr.2007.02.013.

Prego, R., Guzmán-Zuñiga, D., Varela, M., deCastro, M., Gómez-Gesteira, M., 2007. Consequences of winter upwelling events on biogeochemical and phytoplankton patterns in a western Galician ria (NW Iberian peninsula). Estuar. Coast. Shelf Sci. 73: 409–422. http://dx.doi.org/10.1016/j.ecss.2007.02.004.

Relvas, P., Barton, E.D., Dubert, J., Oliveira, P.B., Peliz, Á, da Silva, J.C.B., Santos, A.M.P., 2007. Physical oceanography of the western Iberia ecosystem: Latest views and challenges. Prog. Oceanogr. 74:149–173. http://dx.doi.org/10.1016/j.pocean.2007.04.021.

Ribeiro, A.C., Peliz, Á., Santos, A.M.P., 2005. A study of the response of chlorophyll-a biomass to a winter upwelling event off Western Iberia using SeaWiFS and in situ data. J. Mar. Syst. 53:87–107. http://dx.doi.org/10.1016/j.jmarsys.2004.05.031.

Rodriguez-Puebla, C., Encinas, aH., Nieto, S., Garmendia, J., 1998. Spatial and temporal patterns of annual precipitation variability over the Iberian Peninsula. Int. J. Climatol. 18: 299–316. http://dx.doi.org/10.1002/(SICI)1097-0088(19980315)18:3<299::AID-JOC247>3.0.CO;2-L.

Ruiz Villarreal, M., Bolding, K., Burchard, H., Demirov, E., 2005. Coupling of the GOTM turbulence module to some three-dimensional ocean. Mar. Turbul. Theor. Obs. Model. - Results Cart. Proj. 225–237.

Saha, S., Moorthi, S., Pan, H.-L., Wu, X., Wang, J., Nadiga, S., Tripp, P., Kistler, R., Woollen, J., Behringer, D., Liu, H., Stokes, D., Grumbine, R., Gayno, G., Wang, J., Hou, Y.-T., Chuang, H.-Y., Juang, H.-M.H., Sela, J., Iredell, M., Treadon, R., Kleist, D., Van Delst, P., Keyser, D., Derber, J., Ek, M., Meng, J., Wei, H., Yang, R., Lord, S., Van Den Dool, H., Kumar, A., Wang, W., Long, C., Chelliah, M., Xue, Y., Huang, B., Schemm, J.-K., Ebisuzaki, W., Lin, R., Xie, P., Chen, M., Zhou, S., Higgins, W., Zou, C.-Z., Liu, Q., Chen, Y., Han, Y., Cucurull, L., Reynolds, R.W., Rutledge, G., Goldberg, M., 2010. The NCEP climate forecast system reanalysis. Bull. Am. Meteorol. Soc. 91:1015–1057. http://dx.doi.org/10.1175/2010BAMS3001.1.

Saldías, G.S., Sobarzo, M., Largier, J., Moffat, C., Letelier, R., 2012. Seasonal variability of turbid river plumes off central Chile based on high-resolution MODIS imagery. Remote Sens. Environ. 123:220–233. http://dx.doi.org/10.1016/j.rse.2012.03.010.

Saldías, G.S., Shearman, R.K., Barth, J.A., Tifillaro, N., 2016a. Optics of the offshore Columbia River plume from glider observations and satellite imagery. J. Geophys. Res. Oceans 121:2367–2384. http://dx.doi.org/10.1002/2015JC011431.

Saldías, G.S., Largier, J.L., Mendes, R., Pérez-Santos, I., Vargas, C.A., Sobarzo, M., 2016b. Satellite-measured interannual variability of turbid river plumes off central-southern Chile: spatial patterns and the influence of climate variability. Prog. Oceanogr. 146: 212–222. http://dx.doi.org/10.1016/j.pocean.2016.07.007.

Santos, A.M.P., Peliz, A., Dubert, J., Oliveira, P.B., Angélico, M.M., Ré, P., 2004. Impact of a winter upwelling event on the distribution and transport of sardine (*Sardina pilchardus*) eggs and larvae off western Iberia: a retention mechanism. Cont. Shelf Res. 24:149–165. http://dx.doi.org/10.1016/j.csr.2003.10.004.

Silva, A., Palma, S., Oliveira, P.B., Moita, M.T., 2009. Composition and interannual variability of phytoplankton in a coastal upwelling region (Lisbon Bay, Portugal). J. Sea Res. 62:238–249. http://dx.doi.org/10.1016/j.seares.2009.05.001.

Smyth, T.J., Moore, G.F., Groom, S.B., Land, P.E., Tyrrell, T., 2002. Optical modeling and measurements of a coccolithophore bloom. Appl. Opt. 41, 7679–7688.

Teodoro, A.C., Goncalves, H., Veloso-Gomes, F., Gonçalves, J.a., 2009. Modeling of the douro river plume size, obtained through image segmentation of MERIS data. IEEE Geosci. Remote Sens. Lett. 6:87–91. http://dx.doi.org/10.1109/LGRS.2008.2008446.

Trigo, R.M., DaCamara, C.C., 2000. Circulation weather types and their influence on the precipitation regime in Portugal. Int. J. Climatol. 20, 1559–1581.

Trigo, R.M., Pozo-Vázquez, D., Osborn, T.J., Castro-Díez, Y., Gámiz-Fortis, S., Esteban-Parra, M.J., 2004. North Atlantic oscillation influence on precipitation, river flow and water resources in the Iberian Peninsula. Int. J. Climatol. 24:925–944. http://dx.doi.org/10.1002/joc.1048.

Torres, R., Barton, E.D., 2007. Onset of the Iberian upwelling along the Galician coast. Cont. Shelf Res. 27:1759–1778. http://dx.doi.org/10.1016/j.csr.2007.02.005.

Veloso-Gomes, F., Taveira-Pinto, F., das Neves, L., Pais Barbosa, J., Coelho, C., 2004. Erosion risk levels at the NW Portuguese coast: the Douro mouth - Cape Mondego stretch. J. Coast. Conserv. 10:43. http://dx.doi.org/10.1652/1400-0350(2004)010[0043:ERLATN]2.0.CO;2.

Xie, P., Arkin, P.a., 1997. Global precipitation: a 17-year monthly analysis based on gauge observations, satellite estimates, and numerical model outputs. Bull. Am. Meteorol. Soc. 78:2539–2558. http://dx.doi.org/10.1175/1520-0477(1997)078<2539:GPAYMA>2.0.CO;2.

Yankovsky, A.E., Chapman, D.C., 1997. A simple theory for the fate of buoyant coastal discharges*. J. Phys. Oceanogr. 27:1386–1401. http://dx.doi.org/10.1175/1520-0485(1997)027<1386:ASTFTF>2.0.CO;2.

Ziveri, P., Thunell, R.C., Rio, D., 1995. Export production of coccolithophores in an upwelling region: results from San Pedro Basin, Southern California Borderlands. Mar. Micropaleontol. 24:335–358. http://dx.doi.org/10.1016/0377-8398(94)00017-H.

Zorita, E., Kharin, V., von Storch, H., 1992. The atmospheric circulation and sea surface temperature in the North Atlantic area in winter: their interaction and relevance for Iberian precipitation. J. Clim. 5:1097–1108. http://dx.doi.org/10.1175/1520-0442(1992)005<1097:TACASS>2.0.CO;2.